Continental Shelf Research 285 (2025) 105400

Contents lists available at ScienceDirect

Continental Shelf Research

journal homepage: www.elsevier.com/locate/csr

Namib desert dust affects phytoplankton biomass in the Benguela upwelling region: Insights from first mesocosm study

Monray D. Belelie [a,*], Roelof P. Burger [a], Johanna R.C. von Holdt [b], Rebecca M. Garland [c,d], Gadaffi M. Liswaniso [e], Sandy J. Thomalla [f,g], Stuart J. Piketh [a]

[a] Unit for Environmental Sciences and Management, North-West University, Potchefstroom, North-West, South Africa
[b] Department of Environmental and Geographical Sciences, University of Cape Town, Cape Town, Western Cape, South Africa
[c] Smart Places, Council for Scientific and Industrial Research, Pretoria, Gauteng, South Africa
[d] Department of Geography, Geo-informatics and Meteorology, University of Pretoria, Pretoria, Gauteng, South Africa
[e] Sam Nujoma Marine and Coastal Resources Research Centre, Sam Nujoma Campus, University of Namibia, Henties Bay, Namibia
[f] Southern Ocean Carbon and Climate Observatory, Council for Scientific and Industrial Research, Cape Town, South Africa
[g] Marine Research Institute, Department of Oceanography, University of Cape Town, Cape Town, South Africa

ARTICLE INFO

Keywords:
BUS
Southern African dust
Macronutrients
Trace metals
Chl-a

ABSTRACT

The Benguela upwelling system (BUS) is frequently subject to dust deposition from southern Africa, which supplies macronutrients and trace metals to the ocean. The impact of these nutrients on chlorophyll-a (Chl-a) in the BUS was investigated using the first-ever mesocosm study from 29 September to October 12, 2022. The study employed a single triplicate treatment where mesocosms were seeded with dust (DG) from the Kuiseb ephemeral riverbed, one of the leading dust sources in southern Africa and one unamended control (CM). All mesocosms were also seeded with equal amounts of *Chaetoceros*, *Pavlova*, and *Tetraselmis*, species of phytoplankton commonly found in the BUS. Temporal dynamics in Chl-a, iron (Fe), nitrate (NO_3^-), silicon (Si), orthophosphate (PO_4^{3-}), and light intensity were measured. The data suggests that adding dust from the Namib desert elicited a positive response from the phytoplankton in the BUS, as evidenced by higher Chl-a concentrations in the DG compared to the CM. This study demonstrates the likely importance of southern African dust emission and deposition for phytoplankton productivity in the adjacent BUS.

1. Introduction

Eastern boundary upwelling systems (EBUS) cover only 1% of the Earth's ocean surface, yet they are among the most productive regions globally (Pauly and Christensen, 1995; Carr, 2001; Dansie et al., 2022). The Benguela upwelling system (BUS) is one of these regions located along the west coast of South Africa, Namibia, and Angola between 19 and 34°S (Hutchings et al., 2009). The BUS is in the South Atlantic tropical gyre, known for its high production of diatoms, dinoflagellates, and small flagellates that fuel a lucrative fishing industry (Louw et al., 2016). The BUS is divided into two subsystems (the northern and southern BUS), which are separated by the Lüderitz upwelling cell at 26°S (Duncombe Rae, 2005; Hutchings et al., 2009; Flohr et al., 2014). These two subsystems have different characteristics (in seasonality and variability, etc.), implying that other mechanisms influence them (Hutchings et al., 2009; Verheye et al., 2016). The southern BUS has a seasonal upwelling signal (Hutchings et al., 2009), which peaks in spring (September, October, and November) and summer (December, January, and February) (Shannon and Nelson, 1996; Romero et al., 2003; Hutchings et al., 2009). During this period, the prevailing south-east trade winds and consequent Ekman spiral offshore induces upwelling of nutrient-rich waters that fuels phytoplankton productivity (Shannon, 1985; Lutjeharms and Meeuwis, 1987; Louw et al., 2016). The northern BUS does not express a strong seasonal cycle with more consistent and intense upwelling that is about an order of magnitude larger than the southern BUS counterpart (Rixen et al., 2021). Although the upwelled nutrient-rich waters drive productivity in both the northern and southern upwelling systems, there is a noteworthy difference in the characteristics of phytoplankton productivity (Carr and Kearns, 2003). This difference implies that other factors like phytoplankton fertilisation from dust addition may play a vital role in explaining the differences in productivity (Dansie et al., 2022). Despite high productivity, the region

* Corresponding author.
E-mail address: Monray.Belelie@nwu.ac.za (M.D. Belelie).

https://doi.org/10.1016/j.csr.2024.105400
Received 24 June 2024; Received in revised form 30 December 2024; Accepted 31 December 2024
Available online 31 December 2024

is considered an HNLC region since primary production is less than the potential from upwelled nitrate supply (Capone and Hutchins, 2013). This suggests another factor that is limiting the maximum production capacity. Iron (Fe) has been suggested as a reason for the limited productivity in the BUS (Messié and Chavez, 2015). Dust is vital in transporting biologically essential macronutrients such as nitrogen (N) and phosphorous (P) and micronutrients such as Fe to the ocean in support of primary productivity (Okin et al., 2011). Although the exact biogeochemical role of N, P, and Fe in various marine environments is still uncertain (Achterberg, 2014), the overall contribution of dust to nutrient loading is considered as being crucial for primary productivity in many aquatic systems (Mahowald et al., 2008; Zehr and Kudela, 2011; Bouwman et al., 2013).

According to some estimates, around 477 Tg of dust is emitted from continental sources annually (Mahowald et al., 2010) and transported to oceanic regions. The South Atlantic receives the sixth highest amount at 17 Tg yr^{-}, of which approximately 0.11–0.32 Tg is soluble Fe (Jickells et al., 2005). These dust supplies are generally from human-driven changes in land surfaces, desert regions, and ephemeral dry lakes or riverbeds (Mahowald et al., 2003). Despite these significant dust inputs, research suggests that the main input pathway of Fe is from continental shelves and ocean plateaus through lateral advection and upwelling of sediments (Meskhidze et al., 2007; Chever et al., 2010). However, the previous studies were conducted in subpolar regions far from significant coastal influences, where sediment resuspension and lateral advection are the primary Fe sources. The BUS is different in that it and major dust sources like the Namib desert, which contribute substantial dust inputs to the system (Eckardt and Kuring, 2005; Vickery and Eckardt, 2013). As such, it is not considered a likely contender for Fe limitation of maximum capacity for utilisation of available nitrate. Nonetheless, Dansie et al. (2017a; 2017b, 2022) suggested it as a possibility, but it has not been tested meaningfully. One of the most commonly used methods for testing Fe limitation is to measure the response of phytoplankton to Fe addition in incubation studies (e.g. Liu et al., 2013; Zhang et al., 2018; Zhang et al., 2019).

Similarly, mesocosm experiments that utilise much larger volumes of water to avoid possible bottle effects can also be used to examine phytoplankton's response to dust addition. An example is the positive response in primary productivity to Saharan Desert dust addition observed in the Cretan Sea (Herut et al., 2016; Pitta et al., 2017; Tsagaraki et al., 2017). However, a few studies have observed a negative relationship between dust addition and phytoplankton growth. Some research has shown that metals in aerosols can have a toxic effect on phytoplankton, resulting in negative growth responses (Paytan et al., 2009). This relationship appears species-specific, with *Prochlorococcus* particularly susceptible to Cu or Al toxicity (e.g. the northern Red Sea (Mescioglu et al., 2019) and the western Atlantic (Borchardt et al., 2020). The foremost dust emitters for the BUS are the Makgadikgadi and Etosha pans (Mahowald et al., 2005) and the Kuiseb, Huab, Tsauchab, and Omaruru ephemeral riverbeds, all of which are rich in Fe, N, and P (Dansie et al., 2017b) (with the Huab consisting of 0.5% Copper (von Holdt, 2018)). Despite the potential importance of dust inputs from these sources to the BUS, relatively little is known about the effects of this dust on phytoplankton productivity. A dust monitoring and chlorophyll (Chl-a) remote sensing study (Dansie et al., 2022) has observed enhanced Chl-a concentrations in response to dust deposition events at the daily timeframe, which alludes to the possibility of dust playing an important role. Past research has also investigated the response of phytoplankton to single nutrient treatments of $FeCl_3$ and K_2HPO_4 in the northern BUS (Wasmund et al., 2014), which showed a positive response to P. To our knowledge, the response of phytoplankton from the BUS to a composite dust sample has yet to be investigated. To address this knowledge gap, we conducted the first mesocosm study in the BUS to examine the impacts of Kuiseb riverbed dust on phytoplankton biomass.

2. Materials and methods

2.1. Experimental Design and sampling

The mesocosm study was conducted at the University of Namibia's Sam Nujoma campus (S22°5′42″; E14°15′34″), on the coast of Henties Bay, between 29 September and October 12, 2022 (Fig. 1). Given its location, the town is placed right next to the northern BUS. The campus is situated southwest of the Etosha Pan and Huab riverbeds, northwest of the Kuiseb and Tsauchab riverbeds, and adjacent to the Omaruru riverbed. The experimental setup consisted of four mesocosms made entirely of plastic. One was used as a control mesocosm (referred to as CM), and the other three as the experimental triplicate group subject to dust seeding (referred to as DG (Dust Group): mesocosm experiment EX1, mesocosm experiment EX2, and mesocosm experiment EX3) (Fig. 2).

The mesocosms were cleaned with filtered seawater mixed with granular pool chlorine at 14:00 on 27 September and left until the following day at 09:00 to eliminate any previous experiment residues. The mesocosms were then rinsed twice by flushing with filtered seawater and finally cleaned with a high-pressure cleaner from fresh tap water. The mesocosms were supplied with seawater extracted from 5 to 10 m from the low water mark at <2 m depth during high tide with a plastic hose. Before being introduced into the mesocosms, the seawater underwent filtration through a series of 4 inline filters that ranged from a coarse 25 μm to a fine 1 μm filter (Fig. 3). Each mesocosm was seeded with 2 L of *Chaetoceros*, 1 L of *Pavlova*, and 1 L of *Tetraselmis*. This mix reflects species commonly occurring in the Benguella region, with *Chaetoceros* representing diatoms, *Pavlova* representing haptophytes, and *Tetraselmis* representing Chlorodendrales. The phytoplankton species were added at 16:30 on 28 September and left to mix with the seawater. Turbulence was created in the mesocosms by a constant airflow through plastic pipes at the bottom of each mesocosm to prevent stratification. While this approach ensured homogeneity within the mesocosms, it differs from natural conditions in the BUS, where stratification and variable mixing are common features. These oxygenated conditions likely surpressed key biogeochemical processes such as denitrification and sedimentary Fe mobilisation, potentially underestimating their contributions to nutrient availability. Temperature measurements were taken at 10-min intervals within the mesocosms using three vacuum-sealed Thermochron temperature iButtons distributed within each mesocosm.

Additionally, three temperature iButton sensors were installed outside each mesocosm and programmed to measure ambient temperature at 10-min intervals. The sensors were programmed to store up to 2048 temperature readings at a resolution of ±0.5 °C, with a measurement range of −40 °C–85 °C. To minimise contamination, the tubing used for sampling was secured and not removed between sampling sessions. The exposed ends of the sampling tubes were sealed between each sampling session. All sampling vials were pre-washed with 10% HCl and rinsed thrice with deionised water. Evidence of contamination during sampling or storage was present in the Fe results of day 9 in EX3 (32.57 nM), deemed an outlier and subsequently excluded from further analysis. The initial conditions in the mesocosms were sampled on 29 September at 09:20 after allowing the phytoplankton to mix with the seawater overnight. Dust was added to the experimental mesocosms at approximately 11:00 on the same day. This mixture of 9 g Kuiseb dust and 100 ml seawater was made several hours before the experiment started. Experimental sub-sampling occurred daily at 09:00 for 14 days after the dust addition.

Subsamples for nutrients: total silicate (SiO_4), orthophosphate (PO_4^3), nitrite (NO_2) and nitrate (NO_3) were collected in 100 ml High-Density Polyethylene (HDPE) bottles and stored frozen until analysis. Samples for total Fe samples were passed through a 0.22 μm Millex-GS sterile syringe filter and immediately acidified with 65% HNO_3 (200 μl) under laminar flow in a laboratory. Total Fe and total Si were analysed using

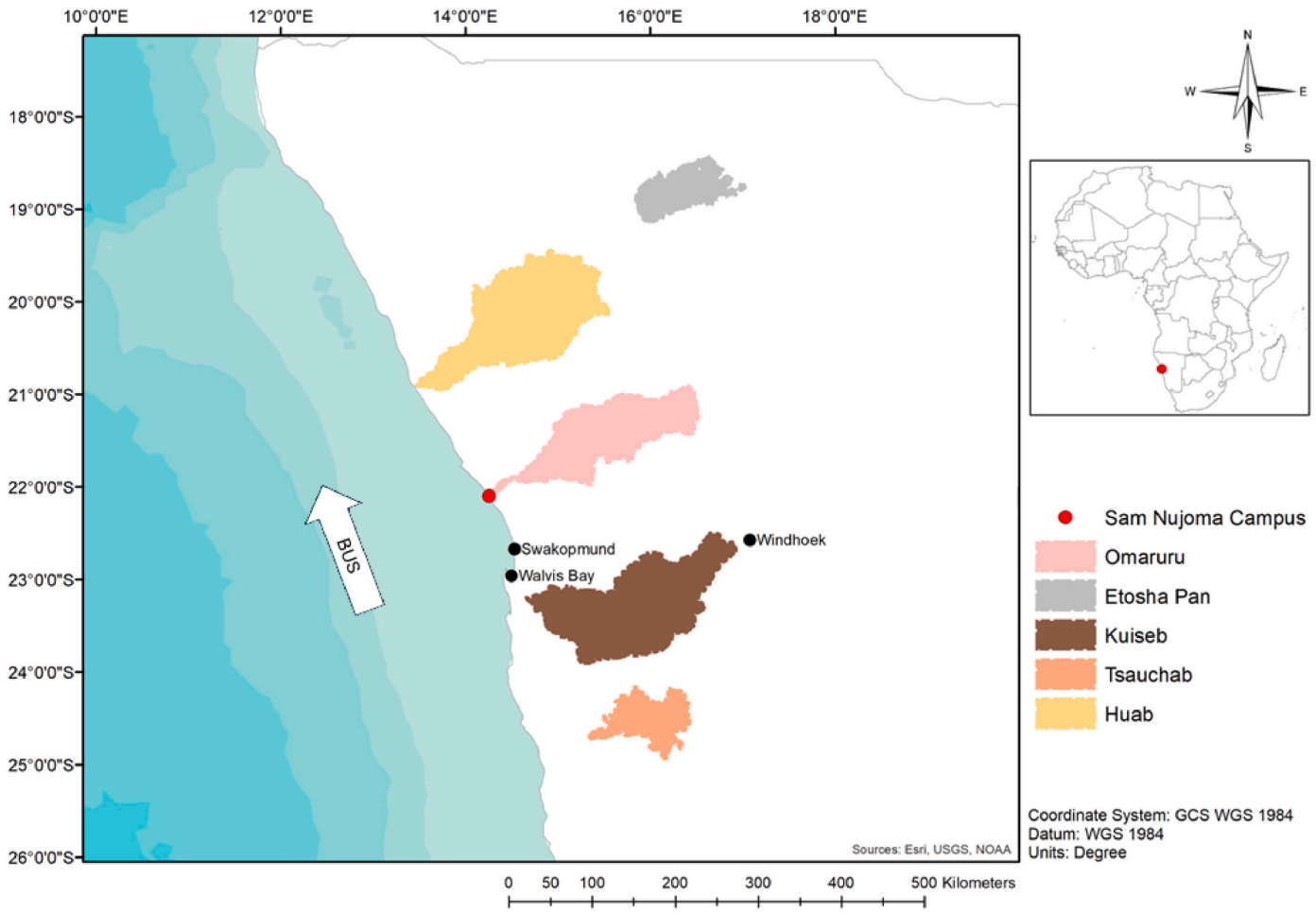

Fig. 1. The location of the Sam Nujoma campus, the northern BUS, and some of the foremost Namibian dust-emitting sources.

Fig. 2. Experimental setup of mesocosms during the experiment. To the far left is the control mesocosm, and right next to it are the three experimental mesocosms that were subject to dust addition.

an aliquot of a homogenised sample that was acid-digested before analysis using inductively coupled plasma optical emission spectroscopy (ICP-OES) (EPA, 1996). NO_2 and PO_4^3 were analysed using a portion of a homogenised sample that was treated with specific reagents before a timed incubation and colour development in Gallery Plus Discrete Analyser (American Public Health Association, 1998). NO_3 was determined by calculating the difference between combined NO_3/NO_2 content and NO_2 content. The syringe filter size of 0.2 μm is recommended as the 0.45 μm filter does not remove all bacteria and plankton (Becker et al., 2020). 500 ml subsamples were collected for Chl-a in glass bottles.

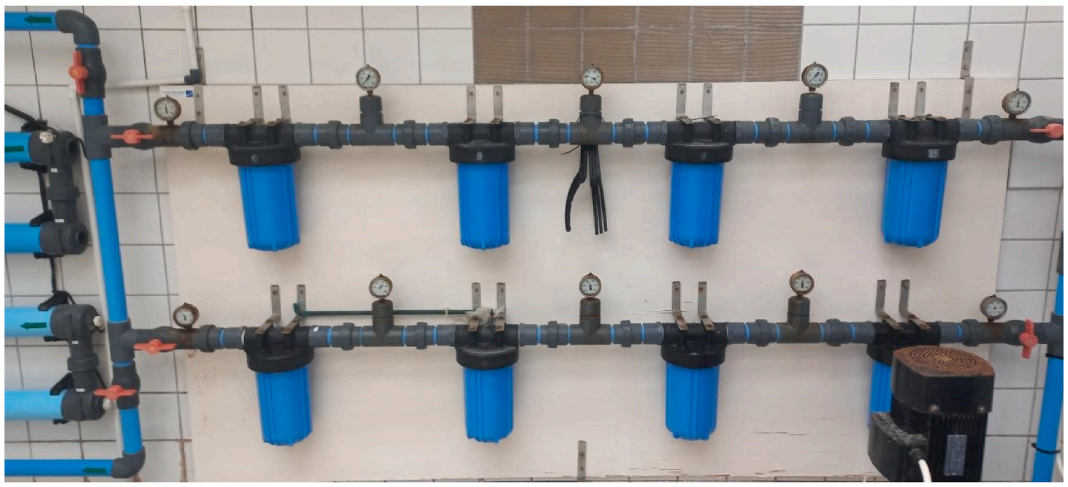

Fig. 3. Filtration system through which seawater was filtered before being pumped into the mesocosms, from right to left: 25 μm, 10 μm, 5 μm and 1 μm.

150 ml of the 500 ml samples were filtered through 47 mm Munktell MGC filters following sampling, and the Chl-a pigment was extracted with 90% acetone (10 ml) for 12–24 h at −20 °C. The Chl-a raw fluorescence was measured with a Turner Trilogy fluorometer and converted to Chl-a concentration using a standard dilution calibration. On the last sampling day, additional Chl-a samples were taken at the mesocosms' front, middle, and back, just below the surface and at the bottom of each mesocosm, to investigate homogeneity. For microscopy, 100 ml of the remaining 350 ml Chl-a samples were stored in brown 100 ml HDPE bottles and preserved with Lugol's solution. After storing for about a week in the dark, cells were counted under a microscope with a Neubauer haemocytometer (0.100 mm depth on a 0.0025 grid) by dispensing 1 ml of the sample. Light intensity inside each mesocosm was measured at noon daily, at the front, back, and middle of each mesocosm with an LI-COR LI-185 B Quantum/Radiometer/Photometer.

2.2. Production of dust

Each mesocosm (1000 L) was supplemented with 9 g of dust from the Kuiseb ephemeral river. The dust samples' particle size distribution, mineralogy, chemical composition, and Fe bioavailability are described elsewhere (Kangueehi, 2017; von Holdt and Eckardt, 2018). Briefly, the samples contained about 57.2 g/kg of Fe, with a solubility of 0.002% atfter 18 h. So as to obtain enough representative dust, soil sediment samples were collected from two transects of an identical terrace and combined to make a composite sample. However, the original composite sample did not yield enough of the <20 μm size fraction. Therefore, the composite sample was crushed with a granite pestle and mortar, and the <20 μm size fraction was enhanced by intense dry-sieving on a vibrating column using three Nylon mesh sheets (20, 40 and 100 μm) for 12–36 h. It has been suggested that this laboratory crushing and sieving of the soil mimics the effects of mechanical wind processes, such as saltation (Guieu et al., 2010). To avoid contamination, all materials used to handle the soil before the experiment were plastic or Nylon, cleaned with 10% HCl and rinsed thoroughly with deionised water. The meshes were cleaned regularly with a brush to prevent clogging.

2.3. Statistical analysis

The statistical significance of the results was assessed using a Levene test to verify the equality of variances between the CM and DG. A Student's t-test was applied for data with equal variance, while a Welch's *t*-test was used for data with unequal variances ($p < 0.05$). Linear regression and ANOVA analysis were performed at $p < 0.05$ to examine the Pearson correlation between Chl-a and each of total Fe, PO_4^{3-}, total Si, and NO_3^- in both CM and DG. For all stations where Fe was below the detection limit, we assigned a maximum value of 2.42 nM by the methodology's detection limit (EPA, 1996). We used these values to calculate the control mean further and plot the temporal changes during the experiment.

All statistical analyses were performed using the open-source pandas v1.5.3, NumPy v1.23.5, and SciPy v1.10.0 packages in Python, with the code developed and tested in the Spyder IDE.

3. Results

3.1. Initial conditions

Before the dust was added at timestep 0, two samples were collected from each mesocosm to establish the initial conditions: one for total Fe and the other for total Si, NO_3^-, NO_2^-, and PO_4^{3-}. The CM had an initial total Fe concentration of 3.87 nM, while the DG had a marginally higher total Fe concentration of 4.3 ± 0.95 nM. The initial total Si concentration was 65.16 nM for the CM and was higher at 86.17 ± 5.33 nM for the DG. The initial NO_3 concentration for both the CM and DG were below the detection limit of 4.03 nM. These concentrations remained below the detection limit for most of the experiment, except for at timestep 3, where the concentration in the CM reached 14.53 nM, possibly due to contamination. For PO_4^{3-}, the initial concentration was 3.79 nM for the CM and 2.60 ± 0.99 nM for the DG. Chl-a concentrations were 3.84 mg/m^3 in the Control mesocosm and 4.94 mg/m^3 in the Dust mesocosm.

3.2. Temporal changes in temperature

During the experiment, the temperature of the seawater varied between 13.5 and 24.5 °C (Fig. 4). Time is in days where Time 0 is the initial conditions before dust addition. The average temperature was calculated from three temperature measurements within each mesocosm. These averages were then calculated across the three DG mesocosms, and the error bar represents the variability in these measurements. Notably, there was a substantial rise in temperature from 06 October until the experiment's conclusion. Although both mesocosms were of a similar temperature at the start (±18 °C), the temperature in the DG was typically 0.63 °C higher than that of the CM for the duration of the experiment. While both mesocosm groups were covered with lids, minimising direct exposure to environmental conditions, the addition of dust in the DG likely contributed to the observed temperature increase. Dust particles, especially larger ones, tend to settle at the bottom of the mesocosms, altering the thermal properties of the water. The presence of dust may have influenced the water's heat retention or conduction,

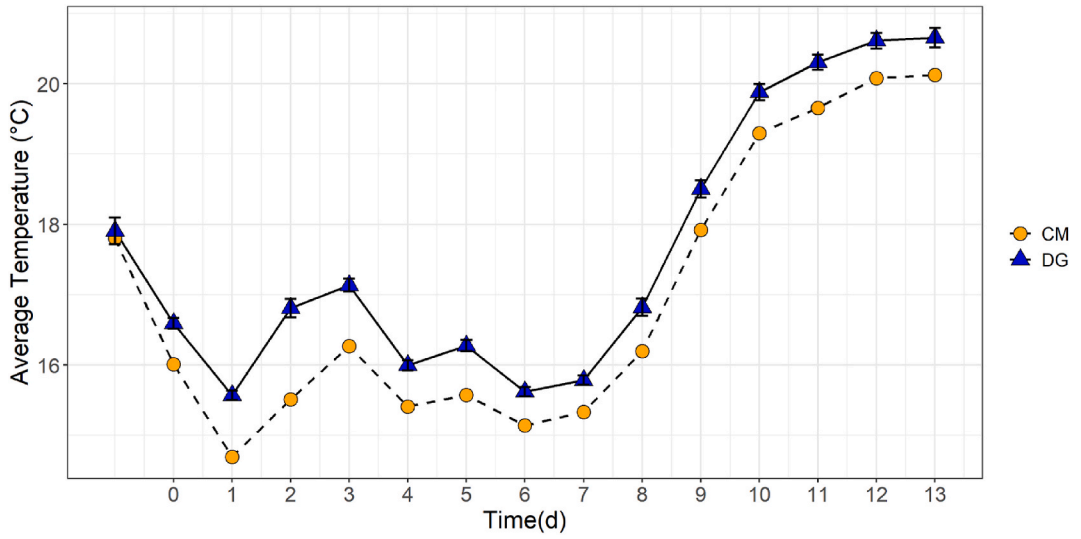

Fig. 4. The temperature evolution in the mesocosms during the experiment. The error bars indicate the standard deviation in the DG group temperatures.

potentially leading to localised warming in the DG. Additionally, the DG could have introduced slight variations in internal dynamics, such as differences in the way heat is distributed or retained, compared to the single CM mesocosm.

3.3. Temporal changes in Chl-a

Chl-a concentrations for both the CM and the DG were relatively low at the start of the experiment, registering values of 3.84 mg/m^3 and 5.03 mg/m^3 and cell densities of 2.05 $\times$ 10^5 cells/ml and 1.61 $\times$ 10^5 cells/ml, respectively (Fig. 5). Chl-a concentrations in both the CM and DG increased steadily from the start of the experiment reaching a maximum at timestep 6 in the CM and timesteps 6–9 in the DG. Notably, maximum concentrations reached in the DG (39.95 $\pm$ 0.64 mg/m^3) were substantially higher and longer lasting than that of the CM (26.55 mg/m^3). Following this, the CM concentration slowly reduced until step 13, ending at 14.15 mg/m^3 and a cell density of 1.35 $\times$ 10^6 cells/ml.

The DG's peak was higher and lasted longer than the CM's peak. However, the DG did reach a second peak at timestep 8 with a slightly higher concentration of 40.04 $\pm$ 5.86 mg/m^3. Following the peak, Chl-a concentrations in both the DG and CM decreased steadily until the end of the experiment (time step 13), ending with a final concentration of 18.79 $\pm$ 1.41 mg/m^3 and 14.15.mg/m^3 in the DG and CM, respectively. At the beginning of the experiment, the Chl-a concentrations were comparable but diverged to a maximum difference of 13.40 $\pm$ 0.79 mg/m^3 at the peak at timestep 6. The maximum difference in Ch-la between the DG and CM was 13.40 mg/m^3, observed during the peak on day 8. A Welch's *t*-test revealed that the experiment means in Chl-a was significantly higher in the DG than the CM ($p < 0.005$).

3.4. Temporal changes in dissolved nutrients

Total Si concentration in both the CM and DG showed considerable day-to-day variation (Fig. 6). Like the CM, the total Si concentration in the DG never depleted completely. Still, it exhibited a more noticeable overall decline over time with some fluctuations. Despite the day-to-day variation, a significant decrease in Si is observed from the fitted trendline for the DG. Although reasonably stable for the first few days, the decline was most evident after day 6, following which it again remained at similar concentrations for the rest of the experiment.

Table 1 presents the correlation and ANOVA results between Chl-a and the considered nutrients and light intensity. None of the

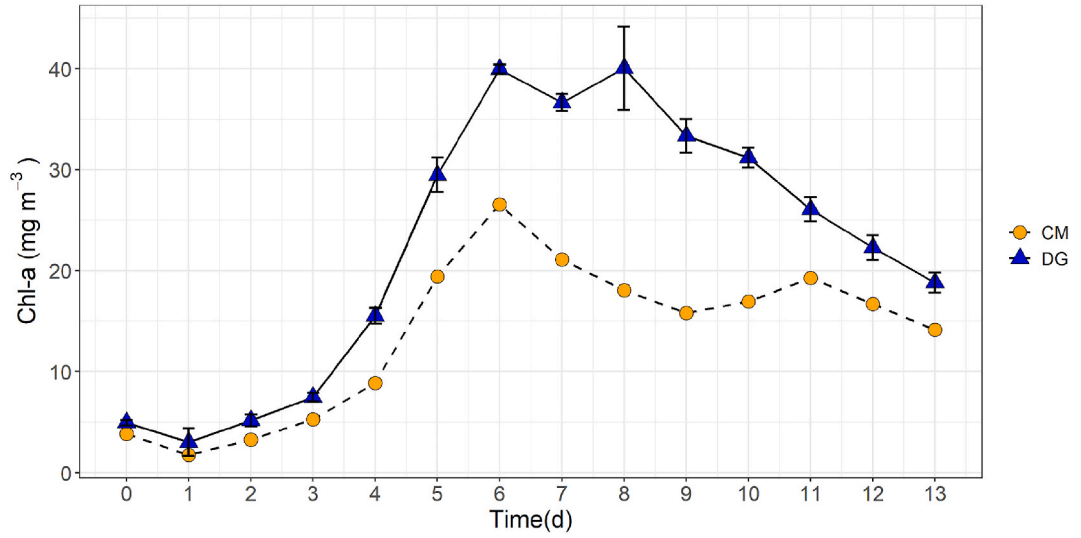

Fig. 5. Chl-a concentration each group for the duration of the experiment. Time (days) = 0 indicates the initial conditions before dust addition, while Time = 1 represents the first measurement taken after dust addition to the DG. The error bars in the graph represent the standard deviation from the mean concentration.

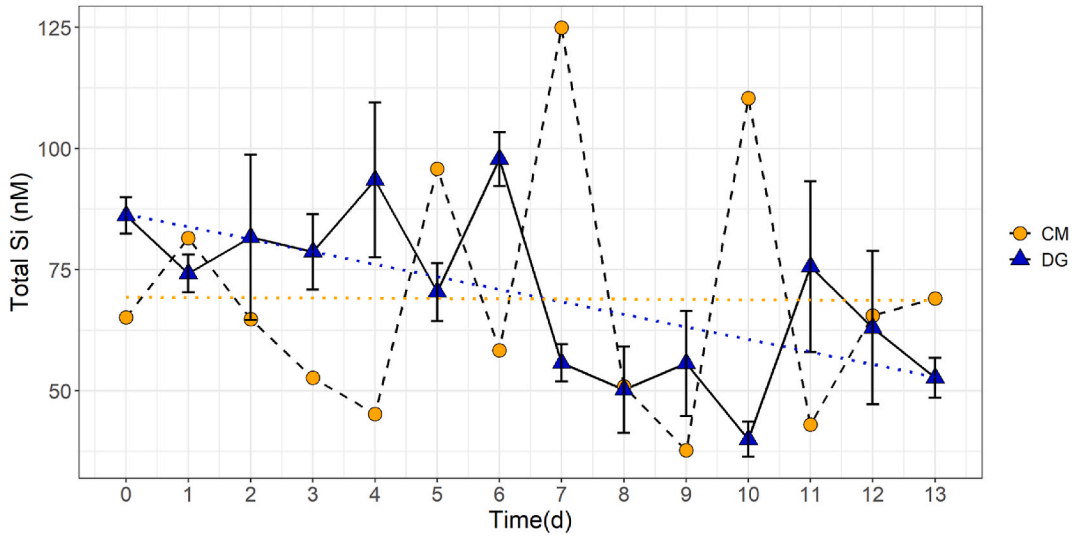

Fig. 6. Total Si concentration in each group for the duration of the experiment. Time (days) = 0 indicates the initial conditions before dust addition, while Time = 1 represents the first measurement taken after dust addition to the DG. The error bars in the graph represent the standard deviation from the mean concentration. The blue and orange trend lines show the general change over time for the DG and CM, respectively. (For interpretation of the references to colour in this figure legend, the reader is referred to the Web version of this article.)

Table 1
Correlation between Chl-a and each nutrient concentration and light intensity during the experiment.

Group	Parameter	Correlation Equation	R^2	F	P	n
CM	total Fe	$y = -5.322x + 27.374$	0.076	0.991	$p > 0.05$	14
	total Si	$y = 0.052x + 10.064$	0.030	0.376	$p > 0.05$	14
	PO_4^{3-}	$y = 0.454x + 10.616$	0.147	2.076	$p > 0.05$	14
	Light intensity	$y = 0.002x + 9.007$	0.063	0.812	$p > 0.05$	14
DG	total Fe	$y = 0.171x + 21.647$	0.004	0.158	$p > 0.05$	13
	total Si	$y = -0.167x + 34.059$	0.080	3.478	$p > 0.05$	14
	PO_4^{3-}	$y = 0.572x + 17.516$	0.041	1.700	$p > 0.05$	14
	Light intensity	$y = 0.004x + 15.416$	0.046	1.937	$p > 0.05$	14

correlations were statistically significant at the 95% confidence level ($p > 0.05$), implying that the observed relationships could have occurred randomly.

PO_4^{3-} concentrations in the CM remained below 6 nM for the first four days of the experiment (Fig. 7). The concentration then gradually rose to 11.16 nM on day 7, followed by a sharp increase to its peak of 26.53 nM on day 8. The concentration then sharply fell to its lowest point of 1.05 nM on day nine and stayed below 6 nM for the rest of the experiment.

No real change was evident in the DG PO_4^{3-} concentrations, which fluctuated between 2.01 and 13.06 nM over the incubation. The most significant fluctuation was an increase from the initial concentration to 12.78 ± 1.01 nM on day 1. After that, the concentrations generally remained stable below 12 nM.

The total Fe concentration in the CM generally stayed beneath the detection limit of 2.42 nM, with minor increases observed on days 8 and 10, where they peaked at 2.9 and 2.74 nM, respectively (Fig. 8). In the DG, the average total Fe concentrations (3.84 ± 2.01 nM) were typically 57.14% higher than those in the CM. Fe concentrations peaked at the start of the time series for the two days after the dust was added (5.21 ± 3.31 nM and 5.21 ± 2.78 nM). Following this, the concentrations dropped on the third day and stayed relatively low for the remainder of the incubation period, ranging from 2.53 ± 0.19 nM to 4.46 ± 2.51 nM.

4. Discussion

The BUS is frequently exposed to substantial aeolian dust inputs from sources such as the Kuiseb, Huab, Tsauchab, and Omaruru ephemeral riverbeds (Vickery and Eckardt, 2013). While these inputs are well-documented, their impact on phytoplankton biomass remains less understood. In our mesocosm experiment conducted near the Namibian continental shelf, where dust deposition and upwelling coexist, it was plausible to expect nutrient-replete conditions for phytoplankton. Despite this, our results revealed significantly ($p < 0.005$) higher Chl-a concentrations in the DG compared to the CM. This response underscores the potential for dust, rich in micronutrients like Fe, to alleviate Fe limitation or stress, thereby enhancing the utilisation of macronutrients such as nitrate. This finding aligns with previous suggestions that Fe can regulate nitrate uptake and productivity in HNLC regions (Messié and Chavez, 2015; Capone and Hutchins, 2013).

The positive response in biomass in the DG was consistent but varied temporally, with Chl-a peaking before declining. This suggests that while Fe supplied by dust may have initially stimulated growth, other limiting factors eventually constrained phytoplankton biomass. Phytoplankton growth can be co-limited by multiple nutrients or influenced by environmental factors, such as light availability, grazing pressure, and nutrient depletion rates (Dubourg et al., 2015). Moreover, the decline in Chl-a following its peak suggests that the Kuiseb dust's low Fe solubility (0.002%; Kangueehi, 2017) could have restricted sustained Fe availability, emphasising the importance of dust bioavailability in mediating phytoplankton responses. Recent research by Desboeufs et al. (2024) highlighted significant variability in the fractional solubility of Fe in dust along the Namibian coast, ranging from 1.3% to 20%, with an average of 7.9% during intense dust events. This variability in Fe solubility provides important context for understanding how Fe release from dust particles fluctuates over time and may influence phytoplankton dynamics in coastal systems.

In natural BUS conditions, dust deposition is only one of many drivers of primary production. Upwelling intensity, which governs the delivery of macronutrients like NO_3^-, PO_4^{3-}, and SiO_4 from deeper waters, remains a dominant control on productivity. Furthermore, the

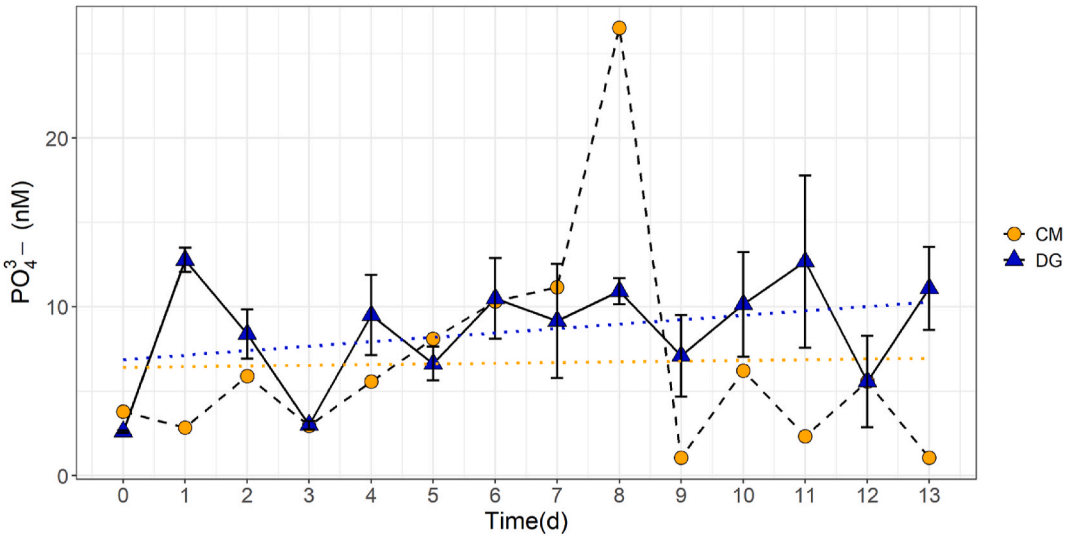

Fig. 7. Concentration of PO_4^3 in each group for the duration of the experiment. Time (days) = 0 indicates the initial conditions before dust addition, while Time = 1 represents the first measurement taken after dust addition to the DG. The error bars in the graph represent the standard deviation from the mean concentration. The blue and orange trend lines show the general change over time for the DG and CM, respectively. (For interpretation of the references to colour in this figure legend, the reader is referred to the Web version of this article.)

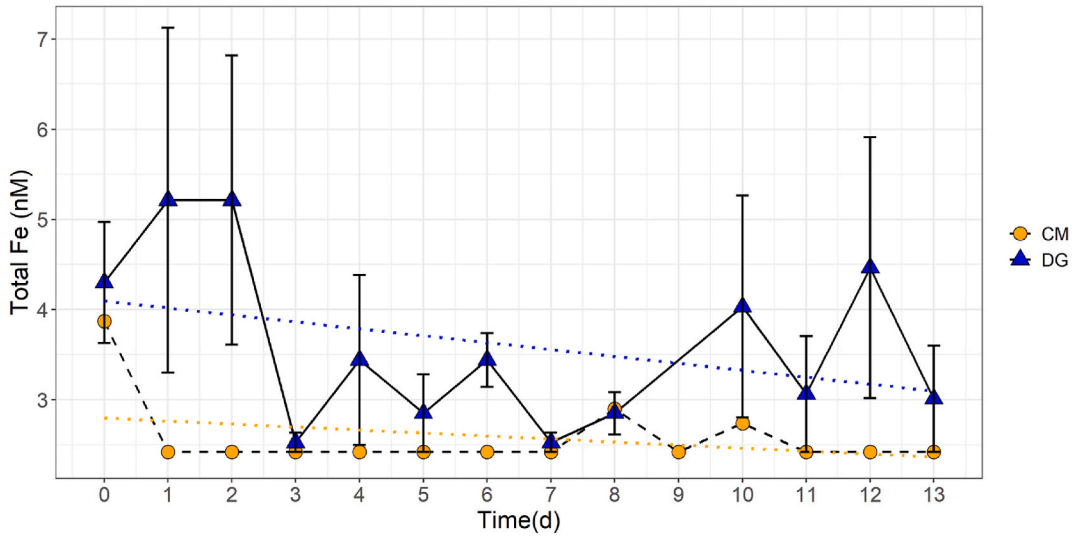

Fig. 8. Total Fe concentration in each group for the duration of the experiment. Time (days) = 0 indicates the initial conditions before dust addition, while Time = 1 represents the first measurement taken after dust addition to the DG. The error bars in the graph represent the standard deviation from the mean concentration. The blue and orange trend lines show the general change over time for the DG and CM, respectively. The minimum data are sensor limits and not measured values. (For interpretation of the references to colour in this figure legend, the reader is referred to the Web version of this article.)

interaction between aeolian Fe supply and upwelling-driven nutrient inputs must be considered. Aeolian dust inputs may act synergistically with upwelled macronutrients, particularly in regions where NO_3 and SiO_4 are abundant but Fe is limiting (Winckler et al., 2016). The influence of water masses, such as the nutrient-rich South Atlantic Central Water (SACW) and the less productive Eastern SACW (ESACW), could also modulate phytoplankton responses by altering baseline nutrient concentrations (Claude, 1993). For instance, SACW is typically associated with higher NO_3^- and SiO_4 levels, which could amplify the effects of dust deposition compared to ESACW-dominated regions (Mohrholz et al., 2008; Lass and Mohrholz, 2005).

The role of additional environmental factors, such as eddies, filaments, and oxygen dynamics, cannot be overlooked. Eddies and filaments can redistribute nutrients and phytoplankton, creating spatial heterogeneity in productivity (Nagai et al., 2015). These features can introduce variability in the distribution of nutrients and affect how phytoplankton respond to dust deposition. In contrast, mesocosm experiments generally lack such dynamic oceanographic features, which means they might not fully capture how these spatial processes influence phytoplankton growth. Oxygen concentrations, including events of hypoxia and anoxia, may influence nutrient cycling and the availability of trace metals like Fe (Ani and Robson, 2021). In the mesocosm setup, oxygen levels are typically regulated and may not reflect the natural fluctuations observed in the open ocean, where oxygen depletion could limit iron availability, even if dust deposition increases nutrient input. In natural systems, periods of low oxygen may negate the benefits of nutrient enhancement from dust, thus reducing productivity despite nutrient availability. Additionally, the pH of the water column, which affects the solubility and speciation of Fe, may play a critical role in determining its bioavailability to phytoplankton (Shi et al., 2010). In

mesocosms, pH is often controlled to mimic typical conditions, but in the natural BUS, fluctuations in pH due to biological activity, upwelling, and carbon chemistry can alter iron bioavailability and influence phytoplankton response to dust. The relationship between dust, nutrients, and phytoplankton growth is thus more complex in the BUS, where pH shifts could limit or enhance iron availability, depending on the prevailing conditions. The interplay between these factors highlights the complexity of transferring mesocosm findings to the natural BUS environment.

Our study also observed an inverse relationship between total Si concentrations and Chl-a, suggesting a potential link between SiO_4 availability and diatom growth. Diatoms like *Chaetoceros* are known to rely heavily on dissolved Si, and their ability to store nutrients during periods of abundance (Salmaso and Tolotti, 2021) may have contributed to their high initial growth rates. The eventual decline in Chl-a concentrations after day eight could indicate Si limitation, consistent with the partial depletion of Si observed in both mesocosms. However, in natural BUS waters, the interplay between dust-derived Fe and upwelled Si may support sustained diatom growth over longer periods, provided other conditions remain favourable (Hutchins et al., 2002).

PO_4^{3-} concentrations in the BUS are generally non-limiting (Flohr et al., 2014), as supported by our observation that PO_4^{3-} levels increased in the DG without constraining phytoplankton growth. Nonetheless, the fluctuations in total Si and PO_4^{3-} during the experiment may reflect the balance between nutrient uptake by growing cells and remineralisation from decomposing phytoplankton (Manzoni et al., 2010; Hattich et al., 2022). The weak correlations between Chl-a and Fe, total Si, PO_4^{3-}, and light suggest that factors beyond these nutrients may drive the variability in phytoplankton biomass. For instance, episodic changes in wind intensity, which influence upwelling strength and nutrient delivery, are known to drive short-term fluctuations in productivity in coastal upwelling systems (Botsford et al., 2006). The authors found that high winds can sometimes reduce new phytoplankton production, which contradicts the assumption that increased upwelling always enhances biological productivity. In other words, in actual BUS conditions, the influence of dust and upwelling on phytoplankton is likely to be modulated by wind intensity, which can cause variability in nutrient availability and phytoplankton growth (Claude, 1993). While the present study's mesocosm results suggest a clear enhancement of phytoplankton growth under dust-enriched conditions, the interaction between upwelling and wind intensity in the BUS means that this relationship may not always be straightforward. High winds could reduce the benefits of nutrient availability, leading to periods of reduced productivity despite the presence of dust.

Although the mesocosm setting provides a controlled environment that isolates the effects of dust on phytoplankton dynamics, it inherently limits the ability to fully replicate the complexity of real-world conditions, such as the influence of zooplankton or deep-water oxygen minimum zones (Meiritz et al., 2024). The observed enhancement of phytoplankton growth under dust-enriched conditions in the mesocosm suggests that dust may indeed influence particle flux by promoting the ballast effect, where the presence of mineral particles like dust increases the sinking rate of organic particles. However, the mesocosm environment likely doesn't fully capture the variability in biological cycles and physical processes, such as resuspension and advective fluxes, that would be present in the open ocean (Francois et al., 2002). In the natural environment, these factors would modulate the contribution of dust to the overall particle flux and biological pump efficiency.

In coastal upwelling systems like the BUS, dust fluxes could be highly variable, influenced by factors such as local biological productivity, oxygen levels, and zooplankton activity, all of which could affect the magnitude and efficiency of the ballast effect (Bory and Newton, 2000; Meiritz et al., 2024). Thus, while the mesocosm experiment provides valuable insights into the potential role of dust in enhancing the sinking rate of organic particles, future studies in natural systems should consider the full range of factors influencing the biological pump, such as upwelling intensity, wind-driven dynamics, and the presence of oxygen minimum zones. It is essential to consider that the mesocosm setup, while informative, represents a simplified system that cannot fully replicate the complexities of the natural BUS. The low solubility of Kuiseb dust Fe observed in our experiment highlights the need for further research on the chemical composition and bioavailability of dust inputs to the BUS. Future studies should also explore the synergistic effects of dust deposition, upwelling, and oceanographic features like eddies and filaments on primary production to better assess the broader implications of dust-derived nutrients for the BUS.

5. Conclusions

One of the critical gaps in knowledge is the exact impact of Namib desert dust on phytoplankton productivity in the BUS. To shed some light on this, this study, for the first time, investigated this relationship in a land-based mesocosm study. The data suggests that adding dust from the Namib desert elicited a positive response from the phytoplankton in the Benguela current, as evidenced by the higher Chl-a concentrations in the DG compared to the CM. The study revealed a significant increase in Chl-a concentrations in response to dust addition in the mesocosm experiments, indicating a potential alleviation of Fe limitation on phytoplankton biomass. While an apparent positive reaction was observed, the temporal variability in biomass suggests multifaceted influences on phytoplankton growth, including factors like bioavailability of Fe and other nutrients such as total Si and PO_4^{3-}. Future research should investigate the mechanisms underlying the observed variability in phytoplankton responses to dust deposition to build on these findings. Investigating the bioavailability of iron and other nutrients in dust samples from different sources, alongside comprehensive nutrient dynamics studies, will provide critical insights.

CRediT authorship contribution statement

Monray D. Belelie: Writing – review & editing, Writing – original draft, Visualization, Methodology, Investigation, Formal analysis. **Roelof P. Burger:** Writing – review & editing, Supervision, Data curation. **Johanna R.C. von Holdt:** Writing – review & editing, Methodology, Conceptualization. **Rebecca M. Garland:** Writing – review & editing, Supervision, Project administration, Funding acquisition, Data curation. **Gadaffi M. Liswaniso:** Writing – review & editing, Methodology, Investigation, Formal analysis. **Sandy J. Thomalla:** Writing – review & editing, Project administration, Methodology, Funding acquisition, Formal analysis, Data curation, Conceptualization. **Stuart J. Piketh:** Writing – review & editing, Supervision, Project administration, Methodology, Funding acquisition, Conceptualization.

Declaration of competing interest

The authors declare that they have no known competing financial interests or personal relationships that could have appeared to influence the work reported in this paper.

Acknowledgements

This research was funded by the National Research Foundation of South Africa (Grant: 120764, 106431, 129320, and 114691).

References

Achterberg, E.P., 2014. Grand challenges in marine biogeochemistry. Front. Mar. Sci. 1, 1–7.

American Public Health Association, 1998. Standard Methods for the Examination of Water and Wastewater, twentieth ed. American Public Health Association, Washington, DC. Method 4500-PG, 4-149 to 4-150.

Ani, C.J., Robson, B., 2021. Responses of marine ecosystems to climate change impacts and their treatment in biogeochemical ecosystem models. Mar. Pollut. Bull. 166, 112223.
Becker, S., Aoyama, M., Malcolm, E., Woodward, S., Bakker, K., Coverly, S., Mahaffey, C., Tanhua, T., 2020. GO-SHIP repeat hydrography nutrient manual: the precise and accurate determination of dissolved inorganic nutrients in seawater, using continuous flow analysis methods. Front. Mar. Sci. 7, 581790.
Borchardt, T., Fisher, K.V., Ebling, A.M., Westrich, J.R., Xian, P., Holmes, C.D., et al., 2020. Saharan dust deposition initiates successional patterns among marine microbes in the Western Atlantic. Limnol. Oceanogr. 65, 191–203.
Bory, A., Newton, P., 2000. The role of atmospheric dust in the biogeochemical cycling of marine elements. Mar. Chem. 69 (1–2), 19–34.
Botsford, L.W., Lawrence, C.A., Dever, E.P., Hastings, A., Largier, J., 2006. Effects of variable winds on biological productivity on continental shelves in coastal upwelling systems. Deep Sea Res. Part II Top. Stud. Oceanogr. 53 (25–26), 3116–3140.
Bouwman, A., Bierkens, M., Griffioen, J., Hefting, M., Middelburg, J., Middelkoop, H., Slomp, C., 2013. Nutrient dynamics, transfer and retention along the aquatic continuum from land to ocean: towards integration of ecological and biogeochemical models. Biogeosciences 10 (1), 1–22.
Capone, D.G., Hutchins, D.A., 2013. Microbial biogeochemistry of coastal upwelling regimes in a changing ocean. Nat. Geosci. 6, 711–717.
Carr, 2001. Estimation of potential productivity in Eastern Boundary Currents using remote sensing. Deep Sea Res. Part II Top. Stud. Oceanogr. 49, 59–80.
Carr, M., Kearns, E.J., 2003. Production regimes in four eastern boundary current systems. Deep-Sea Res. Part II 50, 3199–3221.
Chever, F., Sarthou, G., Bucciarelli, E., Blain, S., Bowie, A.R., 2010. An iron budget during the natural iron fertilisation experiment KEOPS (Kerguelen Islands, Southern Ocean). Biogeosciences 7, 455–468.
Claude, R., 1993. The Optimal Environmental Window Hypothesis. ICES Statutory Meeting, Dublin. Ireland, 19–23 October 1993.
Dansie, A.P., Thomas, D.S.G., Wiggs, G.F.S., Baddock, M.C., Ashpole, I., 2022. Plumes and blooms – locally-sourced Fe-rich aeolian mineral dust drives phytoplankton growth off south-west Africa. Sci. Total Environ. 829, 154562.
Dansie, A.P., Wiggs, G.F.S., Thomas, D.S.G., 2017a. Iron and nutrient content of wind-erodible sediment in the ephemeral river valleys of Namibia. Geomorphology 290, 335–346.
Dansie, A.P., Wiggs, G.F.S., Thomas, D.S.G., Washington, R., 2017b. Measurements of wind-blown dust characteristics and ocean fertilization potential: the ephemeral river valleys of Na-mibia. Aeolian Research 29, 30–41.
Desboeufs, K., Formenti, P., Torres-Sánchez, R., Schepanski, K., Chaboureau, J.-P., Andersen, H., Cermak, J., et al., 2024. Fractional solubility of iron in mineral dust aerosols over coastal Namibia: a link to marine biogenic emissions? Atmos. Chem. Phys. 24 (1), 1–24.
Dubourg, P., North, R.L., Hunter, K., Vandergucht, D.M., Abirhire, O., Silsbe, G.M., Guildford, S.J., Hudson, J.J., 2015. Light and nutrient co-limitation of phytoplankton communities in a large reservoir: lake Diefenbaker, Saskatchewan, Canada. J. Great Lake. Res. 41 (Suppl. 2), 129–143.
Duncombe Rae, C.M., 2005. A demonstration of the hydrographic partition of the Benguela upwelling ecosystem at 26°40'S. Afr. J. Mar. Sci. 27 (3), 617–628.
Eckardt, F.D., Kuring, N., 2005. SeaWiFS identifies dust sources in the Namib Desert. Journal of Remote Sensing 26 (19), 4159–4167.
EPA (Environmental Protection Agency), 1996. Method 6010B: Inductively Coupled Plasma-Optical Emission Spectrometry, Revision 2, December 1992.
Flohr, A., van der Plas, A.K., Emeis, K.-C., Mohrholz, V., Rixen, T., 2014. Spatio-temporal patterns of C : N: P ratios in the Benguela upwelling system. Biogeosci. Discuss. 10, 10459–10489.
Francois, R., Honjo, S., Krishfield, R., Manganini, S., 2002. Factors controlling the flux of organic carbon to the bathypelagic zone of the ocean. Global Biogeochem. Cycles 16 (4), 1087.
Guieu, C., Dulac, F., Desboeufs, K., Wagener, T., Pulido-Villena, E., Grisoni, J.M., Louis, F., et al., 2010. Large clean mesocosms and simulated dust deposition: a new methodolo-gy to investigate responses of marine oligotrophic ecosystems to atmospheric inputs. Biogeosciences 7, 2765–2784.
Hattich, G.S.I., Listman, L., Govaert, L., Pansch, C., Reusch, T.B.H., Matthiessen, B., 2022. Ex-perimentally decomposing phytoplankton community change into ecological and evolutionary contributions. Funct. Ecol. 36, 120–132.
Herut, B., Rahav, E., Tsagaraki, T., Giannakourou, A., Tsiola, A., Psarra, S., Lagaria, A., et al., 2016. The potential impact of saharan dust and polluted aerosols on microbial populations in the east mediterranean Sea, an overview of a mesocosm experimental ap-proach. Front. Mar. Sci. 3, 226.
Hutchings, L., van der Lingen, C.D., Shannon, L.J., Crawford, R.J.M., Verheye, H.M.S., Bartholomae, C.H., et al., 2009. The Benguela current: an ecosystem of four components. Prog. Oceanogr. 83 (1–4), 15–32.
Hutchins, D.A., Hare, C.E., Weaver, R.S., Zhang, Y., Firme, G.F., DiTullio, G.R., et al., 2002. Phytoplankton iron limitation in the humboldt current and Peru upwelling. Limnol. Oceanogr. 54 (4), 1133–1143.
Jickells, T.D., An, Z.S., Andersen, K.K., Baker, A.R., Bergametti, G., Brooks, N., et al., 2005. Global iron connections between Desert Dust, ocean biogeochemistry, and climate. Science 308, 67–71.
Kangueehi, I.K., 2017. Aerosol Trace Metal Concentrations and Dissolution Characteristics from Known Dust Emitters in Southern Africa. Stellenbosch University, Stellenbosch (Thesis – MSc).
Lass, H.U., Mohrholz, V., 2005. On the interaction between the subtropical gyre and the Benguela upwelling system. J. Mar. Syst. 53 (1–4), 87–107.
Liu, Y., Zhang, T.R., Shi, J.H., Gao, H.W., Yao, X.H., 2013. Responses of chlorophyll a to added nutrients, Asian dust, and rainwater in an oligotrophic zone of the Yellow Sea: implications for promotion and inhibition effects in an incubation experiment. J. Geophys. Res.: Biogeosciences 118, 1763–1772.
Louw, D.C., van der Plas, A.K., Mohrholz, V., Wasmund, N., Junker, T., Eggert, A., 2016. Sea-sonal and interannual phytoplankton dynamics and forcing mechanisms in the Northern Ben-guela upwelling system. J. Mar. Syst. 157, 124–134.
Lutjeharms, J.R.E., Meeuwis, J.M., 1987. The extent and variability of South-East Atlantic upwellings. S. Afr. J. Mar. Sci. 5, 51–62.
Mahowald, N., Jickells, T.D., Baker, A.R., Artaxo, P., Benitez-Nelson, C.R., Bergametti, G., Bond, T.C., et al., 2008. Global distribution of atmospheric phosphorous sources, concentrations and deposition rates, and anthropogenic impacts. Global Biogeochem. Cycles 22 (4).
Mahowald, N.M., Baker, A.R., Bergametti, G., Brooks, N., Duce, R.A., Jickells, T.D., et al., 2005. Atmospheric global dust cycle and iron inputs to the ocean. Global Biogeochem. Cycles 19 (4), GB4025.
Mahowald, N., Luo, C., de Corral, J., Zender, C., 2003. Interannual variability in atmospheric mineral aerosols from a 22-year model simulation and observational data. J. Geophys. Res. 108, 4352.
Mahowald, N.M., Kloster, S., Engelstaedter, S., Moore, J.K., Mukhopadhyay, S., McConnell, J.R., Albani, S., et al., 2010. Observed 20th century desert dust variability: impact on cli-mate and biogeochemistry. Atmos. Chem. Phys. 10, 10875–10893.
Meiritz, L.C., Rixen, T., van der Plas, A.K., Lamont, T., Lahajnar, N., 2024. The influence of zooplankton and oxygen on the particulate organic carbon flux in the Benguela Upwelling System. Biogeosciences 21, 5261–5276.
Manzoni, S., Trofymow, J.A., Jackson, R.B., Porporato, A., 2010. Stoichiometric controls on car-bon, nitrogen, and phosphorus dynamics in decomposing litter. Ecological Mongraphs 80 (1), 89–106.
Mescioglu, E., Rahav, E., Frada, M.J., Rosenfeld, S., Raveh, O., Galetti, Y., et al., 2019. Dust-associated airborne microbes affect primary and bacterial production rates, and eukaryotes diversity, in the northern Red Sea: a mesocosm approach. Atmosphere 10 (7), 358.
Meskhidze, N., Nenes, A., Chameides, W.L., Luo, C., Mahowald, N., 2007. Atlantic southern ocean productivity: fertilization from above or below? Global Biogeochem. Cycles 21, GB2006.
Messié, M., Chavez, F.P., 2015. Seasonal regulation of primary production in eastern boundary upwelling systems. Prog. Oceanogr. 134, 1–18.
Mohrholz, V., Bartholomae, C.H., van der Plas, A.K., Lass, H.U., 2008. The seasonal variability of the northern Benguela undercurrent and its relation to the oxygen budget on the shelf. Continent. Shelf Res. 28 (3), 424–441.
Nagai, T., Gruber, N., Frenzel, H., Lachkar, Z., McWilliams, J.C., Plattner, G.-K., 2015. Dominant role of eddies and filaments in the offshore transport of carbon and nutrients in the California Current System. J. Geophys. Res.: Oceans 120 (6), 4085–4103.
Okin, G.S., Baker, A.R., Tegen, I., Mahowald, N.M., Dentener, F.J., Duce, R.A., Galloway, J.N., et al., 2011. Impacts of atmospheric nutrient deposition on marine productivity: roles of ni-trogen, phosphorus, and iron. Global Biogeochem. Cycles 25 (2).
Pauly, D., Christensen, V., 1995. Primary production required to sustain global fisheries. Nature 374, 255–257.
Paytan, A., Mackey, K.R.M., Chen, Y., Lima, I.D., Doney, S.C., Mahowald, N., et al., 2009. Toxicity of atmospheric aerosols on marine phytoplankton. Proc. Natl. Acad. Sci. USA 106 (12), 4601–4605.
Pitta, P., Kanakidou, M., Mihalopoulos, N., Christodoulaki, S., Dimitriou, P.D., Frangoulis, C., et al., 2017. Saharan dust deposition effects on the microbial food web in the eastern mediterranean: a study based on a mesocosm experiment. Front. Mar. Sci. 4, 117.
Rixen, T., Lahanjar, N., Lamont, T., Koppelmann, R., Martin, B., Beusekom, J.E.E., Siddiqui, C., et al., 2021. Oxygen and nutrient trapping in the southern Benguela upwelling system. Front. Mar. Sci. 8, 730591.
Romero, O., Mollenhauer, G., Schneider, R.R., Wefer, G., 2003. Oscillations of the siliceous im-print in the central Benguela upwelling system from MIS 3 through to the early holocene: the influence of the southern ocean. J. Quat. Sci. 18 (8), 733–743.
Salmaso, N., Tolotti, M., 2021. Phytoplankton and anthropogenic changes in pelagic environ-ments. Hydrobiologia 848, 251–284.
Shannon, L.V., 1985. The Benguela Ecosystem Part I: evolution of the Benguela, physical features and processes. Oceanogr. Mar. Biol. 23, 105–182.
Shannon, L.V., Nelson, G., 1996. The Benguela: large scale features and processes and system variability. In: Wefer, G., Berger, W.H., Siedler, G., Webb, D.J. (Eds.), The South Atlantic: Present and Past Circulation, pp. 163–210.
Shi, D., Xu, Y., Hopkinson, B.M., Morel, F.M.M., 2010. Effect of ocean acidification on iron availability to marine phytoplankton. Science 327 (5966), 676–679.
Tsagaraki, T.M., Herut, B., Rahav, E., Berman-Frank, I.R., Tsiola, A., Tsapakis, M., et al., 2017. Atmospheric deposition effects on plankton communities in the eastern mediterranean: a mesocosm experimental approach. Front. Mar. Sci. 4, 210.
Verheye, H.M., Lamont, T., Huggett, J.A., Kreiner, A., Hampton, I., 2016. Plankton productivity of the Benguela current large marine ecosystem (BCLME). Environmental Development 17, 75–92.
Vickery, K.J., Eckardt, F.D., 2013. Dust emission controls on the lower Kuiseb river valley, cen-tral Namib. Aeolian Research 10, 125–133.
von Holdt, J.R.C., 2018. Aeolian Dust Emission Dynamics across Spatial Scales: Landforms, Controls and Characteristics. University of Cape Town, Cape Town (Thesis – PhD).
von Holdt, R., Eckardt, F.D., 2018. Dust activity and surface sediment characteristics of the dusti-est river in southern Africa: the Kuiseb River, Central Namib. S. Afr. Geogr. J. 100 (1), 104–121.

Wasmund, N., Nausch, G., Hansen, A., 2014. Phytoplankton succession in an isolated upwelled Benguela water body in relation to different initial nutrient conditions. J. Mar. Syst. 140, 163–174.
Winckler, G., Anderson, R.F., Eglinton, T.I., 2016. Aeolian dust inputs and their influence on marine productivity. Nat. Commun. 7, 12345.
Zehr, J.P., Kudela, R.M., 2011. Nitrogen cycle of the open ocean: from genes to ecosystems. Ann. Rev. Mar. Sci 3, 197–225.
Zhang, C., Gao, H., Yao, X., Shi, Z., Shi, J., Yu, Y., Meng, L., Guo, X., 2018. Phytoplankton growth response to asian dust addition in the northwest pacific ocean versus the yellow Sea. Biogeosciences 15, 749–765.
Zhang, C., Yao, X., Chen, Y., Chu, Q., Yu, Y., Shi, J., Gao, H., 2019. Variations in the phytoplankton community due to dust additions in eutrophication, LNLC and HNLC oceanic zones. Sci. Total Environ. 669, 282–293.